JOINT EUROPEAN TORUS JET

JET–P(93)76

V.P. Bhatnagar, J. Jacquinot

A Wide-Band ICRF Antenna for the Next-Step Tokamak

A Wide-Band ICRF Antenna for the Next-Step Tokamak

V.P. Bhatnagar, J. Jacquinot

JET-Joint Undertaking, Culham Science Centre, OX14 3DB, Abingdon, UK

Preprint of a paper to be submitted for publication in
Nuclear Fusion (letters)
October 1993

A WIDE-BAND ICRF ANTENNA FOR THE NEXT-STEP TOKAMAK

V.P. Bhatnagar, J. Jacquinot

JET Joint Undertaking, Abingdon, OXON, OX14 3EA (U.K.)

ABSTRACT.

The flexibility provided by a variety of ion-cyclotron resonance heating (ICRH) and current drive (CD) scenarios for ITER requires that the antenna should operate at a number of frequencies spread over a wide frequency range (20-85 MHz). A new concept of the traditional short-circuited strip-line antenna is presented in which a long strap is connected in parallel with a very short section. The latter acts as a matching element located within the antenna and improves the power coupling capability especially at low frequencies where the plasma coupling is generally poor. The short section also supports the feed-line central conductor. This allows to dispense with the need of a ceramic support in the immediate vicinity of the antenna that will be subjected to a harsh neutron environment in a reactor.

1. INTRODUCTION.

A variety of ICRF scenarios [1,2] have been proposed for the current drive and heating of a next-step tokamak device such as the International Thermonuclear Experimental Reactor (ITER) which is presently in its phase of Engineering Design Activity (EDA). At the design value of toroidal field $B_\phi = 6$ T on axis of ITER-EDA, ICRF operation at a number of frequencies (for example, $f \cong 22$, 43, 60, 75 and 85 MHz; see Table 1) is desirable. The analysis of an antenna resonating at a single frequency midway in the 20-85 MHz band is found to give rise to excessive voltages (>60 kV) in the feeding line, to couple a given 2 MW of power per unit, especially at the lower end of the frequency band. Therefore, there is a need to improve the band width of the antenna that is obtained by the conventional design used presently.

The ICRF antennas operating in the present generation of tokamaks use conventional short-circuited strip-line configurations. Although, multiple straps in the toroidal direction (for example, for current drive phasing) are used, a strap at a given toroidal location consists of either two strip-lines connected in parallel resonating at a single frequency, for example, JET [3], ASDEX-Upgrade [4], or a single strip-line TEXTOR [5], DIII-D [6], or two strip lines with their short circuits connected back-to-back TFTR [7], JT60-U [8]. However, on TORE-Supra [9], a compact loop antenna design previously developed at ORNL [10], is used. In the latter design, each antenna loop is fed by a current tap that is offset slightly from the centre of the loop with variable vacuum capacitors terminating each end of the loop. These capacitors serve the purpose of tuning the antenna but often can lead to reliability problems related to high voltages in these lumped elements. With a view

to developing a wide-band ICRF antenna for ITER, in this paper, we propose to use a long ($L_1 \cong 2.6$m) strip line, short-circuited at its far end and loaded with a distributed capacitance (conveniently provided by a electrostatic screen) such that it exhibits its multiple resonances (at $L_1 = n\lambda/4$, $n = 1,3...7$) in the frequency band mentioned above. However, to improve the matching at the lower end of the frequency band, we connect a short section of strip-line in parallel ($L_2 \cong L_1/7$). The latter also short-circuited (connected to mass at its other end) serves twofold purposes: (i) it partially cancels the reactive part of the admittance of the main long-loop and (ii) it provides a solid support for the central conductor of the feed line thereby eliminating the need of a problematic ceramic support near the antenna in the harsher neutron environment of a reactor. Such a configuration allows coupling of ICRF power to the plasma in a wide range of frequencies keeping maximum voltages on the antenna and the feed-line well within the acceptable (< 40kV) range for a realistic radiation resistance in the presence of the plasma. In section 2, we present a simpified theoretical analysis of the proposed antenna configuration. In section 3, the results of this analysis are given. The discussion and conclusions of this paper are contained in section 4.

2. THEORETICAL ANALYSIS.

2.1 General Remarks: A traditional ICRH antenna consists of one or more sections of short-circuited strip-lines which is surrounded by an electrostatic shield made of an array of metal rods (see Fig. 1). Analysis of the excitaion of fast magnetosonic waves (dominant polarization E_y, B_z) by such an ICRH antenna in a tokamak plasma is well known [11,12]. It is generally treated by a full-wave solution in the context of a semi-infinite planar model under single pass absorption conditions. The slow wave (E_z, B_y) is assumed to be filtered out by the electrostatic screen especially in view of the fact that in the most modern screen designs, the shield rods are aligned to the direction of the total magnetic field. Application of the induced emf method to the solution of this boundary value problem of the antenna-plasma coupling (see, for example Ref. 13) leads to the specific (per unit length) radiation resistance (R_r), inductance (L_{ST}) and capacitance (C_{ST}) of the strip-line antenna. However, from the engineering point of view, there is a need to relate this R_r or the plasma loading of the strip-line antenna to another important quantity, the so-called coupling resistance R_c [14], so that the practical quantities such as the voltage and current on the feeder line and the antenna, to couple a given amount of power, can be determined. Note that at a given frequency of operation, R_r depends on the antenna dimensions such as d and the excitation of $k_{//}$-spectrum (W_{ZF} or the gap L_Z between several toroidally separated energized straps), as well as the proximity of the plasma to the antenna, the plasma edge density and the scrape-off length etc. However, the coupling resistance R_c includes the effects not only of R_r, but also the properties of the feeder line as it is defined by $R_c = Z_{0L}/s$ where Z_{0L} is the characteristic impedance of the feeder line and s is the voltage standing wave ratio (VSWR) in the line. The quantity s is determined from the magnitude of the reflection coefficient at the point where the feeder connects the antenna and thus requires the antenna input impedance determined from the lossy strip-line antenna parameters (R_r,L_{ST} and C_{TOT}) where C_{TOT} includes C_{ST} and the additional capacitance (C_{ADD})

provided by the screen. For the purpose of this paper, we will not repeat the solution of the antenna plasma coupling problem. However, using the coupling code (BRACCO) [11,13], we will present an example of the typical variation of R_r and inductance as a function of frequency (see also Ref. 14) and expressions to fit these two quantities as a function of frequency will be extracted. To evaluate the characteristics of the new antenna design, our main task is to compute the voltages and currents on the antenna and the feeder as a function of frequency for a given power to be delivered. Therefore, in this paper, we will mainly concern ourselves with the calculation of R_c as a function of frequency. For this purpose, plasma effects are included in the framework of the so called 2D-model [11,13], assuming that the antenna is infinitely long. The plasma provides a radiation resistance $R_r(\Omega/m)$ that increases with frequency but the inductance is almost independent of frequency.

2.2 Strip-line Antenna Analysis: Without the screen, the strip line configuraion shown in Fig. 1 supports the transverse electromagnetic waves ($TEM|_y$, refering to the y-direction) [15] provided that $k_0 d \ll 1$ where d is the distance between the two plates, $k_0 = \omega/c$ and c is the velocity of light. These waves propagate nearly at the speed of light in vacuum and $\beta = k_0 = \omega\sqrt{L_{ST}C_{ST}}$ where L_{ST} and C_{ST} are the inductance and capacitance per unit length of the strip line. However, by the addition of a distributed capacitance such as that provided by a electrostatic screen, the phase velocity of the waves can be reduced. Since this parameter is somewhat under the designer's control, we define a parameter $\beta_0 = c/v_p$ and $\beta = \beta_0 k_0$ where $v_p = \omega/\beta$.

The antenna input admittance Y_A at the point A of the two parallel strip-lines of length L_1 and L_2 short-circuited at their far ends is simply [15],

$$Y_A = Y_{1A} + Y_{2A} \tag{1}$$

where

$$Y_{iA} = Y_{0A} \bullet \coth\gamma L_i; i = 1,2 \tag{2}$$

and

$$Z_{0A} = 1/Y_{0A} = \sqrt{(R_r + j\omega L_{ST})/j\omega C_{TOT}} \tag{3}$$

and

$$\gamma = \sqrt{(R_r + j\omega L_{ST}) \bullet j\omega C_{TOT}} \tag{4}$$

where $\gamma = \alpha + j\beta$ is is the complex propagation constant, R_r is the antenna radiation resistance and C_{TOT} includes C_{ST} and the additonal capacitance C_{ADD} provided by the electrostatic screen. Note that the conductance G in the intervening medium between the strip-line is assumed to be negligibly small. When this antenna is connected to a generator via a low-loss coaxial transmission line of characteristic impedance of Z_{0L}, we can define a reflection coffecient in the transmission line as

$$\rho = (1 - Z_{0L} \bullet Y_A)/(1 + Z_{0L} \bullet Y_A) \tag{5}$$

The coupling resistance that can be easily measured experimentally as mentioned above, is defined as $R_c = Z_{0L}/s$ where s is the VSWR. The value of R_c can be described as the value of the antenna resistance seen at a current antinode in the feeder transmission line. Further, we have

$$R_c = Z_{0L} \cdot (1 - |\rho|)/(1 + |\rho|) \tag{6}$$

To couple a given amount of RF power P_T, the maximum voltage in the feeder line is given by,

$$V_{max}^2 = 2P_T \cdot Z_{0L}^2/R_c$$

The maximum voltage and current in the strip line sections and their variation along their lengths can be easily calculated using transmission line formulae for short circuited sections for a given power P_T coupled to the antenna [15] and are as follows:

$$V_i(x) = V_A \cdot (\sinh \gamma_i x / \sinh \gamma_i L_i) \tag{7}$$

$$I_i(x) = (V_A/Z_{0Li}) \cdot (\sinh \gamma_i x / \sinh \gamma_i L_i) \tag{8}$$

$$P_i = 0.5\mathrm{Re}(Y_{iA} V_A^2) \tag{9}$$

and the total power $P_T = \Sigma P_i$.

As input parameters, we take β_0 and R_{0A}, the real part of antenna characteristic impedance Z_{0A}. We now calculate the inductance and the total capacitance of the loaded strip line as follows:

$$L_{ST} = \beta_0 \cdot R_{0A}/c$$

$$C_{TOT} = \beta_0/(R_{0A} \cdot c)$$

Using the Lecher line formulas [16], we can calculate the required ratio r of the width (W_{ZF}) to the gap (d) of the strip line. The value of d is determined from the antenna plasma coupling considerations (such as distance to the plasma, edge density, scrape-off lengths etc). Given d, the value of W_{ZF} is obtained from r. For this value of r, Lecher line formulas are also used to calculate the capacitance C_{ST} contributed by the strip-line. The additional distributed capacitance required $C_{ADD} = C_{TOT} - C_{ST}$ is then to be provided by the electrostatic screen and/or by appropriately placed metallic structures near the central conductor of the strip line. Thus, for given lengths of the two strip-line sections in parallel, given their R_{0A}, β_0, the radiation resistance R_r and the chosen Z_{0L}, the following quantities, the input impedance, coupling resistance and voltages and currents in the antenna and the feeding line can be calculated from the formulas given above. Note that this analysis can be easily extended to include any number of antenna straps in parallel.

3. COMPUTED RESULTS.

We now illustrate the results of a calcualtion using the analysis presented in the previous section. Our aim is to show that a wide band antenna for ITER can be designed so that the frequency response of the coupling resistance has reasonably high values at frequencies that are dictated by the numerous fast-wave current drive and heating scenarios mentioned in section 1. Higher values of R_c ($> 9\Omega$) allows to keep the voltage in the feed-line to comfortable values (< 28kV), at the required frequencies of operation, to couple a given amount of power ($\cong 4$MW) with a $Z_L = 30\Omega$

For illustration, we choose the length of two sections as $L_1 = 2.6$m and $L_2 = 0.4$m. Taking into account the effect of a typical ITER plasma (see Fig. 2) in the reduction of the strip line inductance, $R_{0A} = 46.4\Omega$ and $\beta_0 = 2.9$ results in the antenna width $W_{ZF} = 0.20$m for a value of $d = 0.25$ m and the electrostatic screen distance $X_{SC} = 0.01$m.

3.1 Radiation Resistance: Using the 2-D antenna-plasma coupling code BRACCO [11,13], we calculate the radiation resistance of an antenna with the above dimensions that is coupled to an ITER-EDA like plasma and calculate R_r as a function of frequency. The results of such a calculation from which the vacuum radiation has been subtracted out is given in Fig. 2 where two straps toridally separated by a distance of 0.94 m were phased in the dipole $(0, \pi)$-phasing. Also, we have taken the antenna plasma distance $a = 0.2$m and the density scrape-off length $\lambda_n = 0.02$m. Other parameters used in the calculation are given in the figure caption. We note that R_r increases with frequency and is related to the reduction in the evanescent layer as $k_\perp$ increases with frequency. This increase can be parametrised by fitting the calculated values in the range 20-85 MHz by the following expression

$$R_r(\Omega/\text{m}) = R_{r0}(\Omega/\text{m}) \bullet \exp(\alpha_f \bullet f(\text{MHz})) \qquad (10)$$

where f is the frequency of operation in MHz. Fitting the above relation with the calculated values we found that the values of $R_{r0} = 2.5\Omega$/m and the coefficient $\alpha_f = 0.02$, represent well the variation of R_r in the frequency domain used in our calculations.

3.2 Coupling Resistance: Using the value of R_r parameterised above to include the effects of plasma coupling in our simplified analysis (Eqs 1-9) of strip-line antenna, in Fig.3, we show the the antenna coupling resistance as a function of frequency for two cases: (i) two straps in parallel with $L_1 = 2.6$m and $L_2 = 0.4$m and (ii) for comparison with only one strap of length $L = 2.6$m. Note that there are four peaks in R_c in the frequency domain of interest. The peaks in R_c occur when $|\rho|$ is minimum. In the one strap case, this happens when the electrical length of the strip-line $\beta L \cong n\pi$ where $n = 1,2...$ etc. The value of R_c at this frequencies is then governed by s which is simply determined by Z_{0L} and R_c.

In the case when another short strap is connected in parallel to the previous long strap, the first three peaks shift to lower frequencies while the fourth to a higher frequency. The presence of the short section contributes to an additional admitance at the point A as shown in Fig. 4. The peaks in R_c as before are governed by the $|\rho|$ determined by the complex input admittance at the point A. These are now found at frequencies where $Re(Y_A) \cong Re(Y_{0L})$ which occurs at frequencies somewhat smaller than those in the case of a single strap, since at these frequencies, Im (Y_{2A}) partially cancels the $Im(Y_{1A})$. This cancellation is akin to a stub matching and it has a dramatic effect in improving R_c at the lowest peak albeit making it narrow and somewhat degrading R_c at nearby frequencies. Similar behaviour occurs at second and third peaks. Note that for the fourth peak, the cancellation of $Im(Y_{1A})$ occurs beyond the $\lambda/2$ resonance.

3.3 Voltage, Current and Radiated Power: The maximum voltage $|V_{max}|$ and the maximum current $|I_{max}|$ in the feeder line and the antenna are given in Fig. 5 and 6 respectively. Note that the $|V_{max}|$ is below 40 kV both on the antenna and the feeder line in the entire frequency band. However, when comparing with a single strap, at the desired frequencies of 22 and 43 MHz, the $|V_{max}|$ feeder-line voltage has been considerably lowered whereas the $|V_{max}|$ on the antenna, as expected, is only marginally improved. A similar comparison (not shown) with a conventional antenna configuration of symmetrical splitting (2 sections of equal lengths 1.5m each) shows that fewer peaks in R_c occur in the same frequency band as the line length is shorter. But, the $|V_{max}|$ feeder-line voltage is considearbly worse at low frequencies when compared to asymmetrically split antenna.

The power radiated by the two sections of the antenna are shown in Fig. 7 where it is seen that major part of the power is radiated by the long section. The short section not only improves the match (hence increases R_c) and lowers the voltage on the feeder-line but also contributes to significant power radiation at some frequencies.

For illustration, the variation of voltage and current on the two sections of the antenna are shown in Fig. 8 at a frequency of 23.5 MHz. The voltage goes down to zero at the short-circuit ends of both sections where the antenna currents are maximum. The voltage at the input point of the two parallel sections are equal whereas the currents are as shown. Note that at this frequency the electrical length of the antenna is close to $\lambda/2$ and the two antinodes of the current are separated by a node roughly in the middle and the current reverses on the antenna as shown. This has some consequences on the excitaion of poloidal mode numbers and the antenna-plasma coupling.

3.4 Radiated Power Spectrum: When the electric length of the antenna is $> \lambda/4$, current flowing in the y-direction (poloidal) reverses sign depending on the number of times the current nodes appear on the antenna. In the case of Fig. 8, we have made a full 3-D finite lenth antenna plasma coupling calculation [11] using such a current distribution at f = 23.5 MHz. We compare this result with that at f = 10 MHz where the electric length is $< \lambda/4$ and there is no current reversal. The calculated radiated power spectrum as a function of the poloidal mode number (integrated over all $k_{//}$) is shown in Fig. 9. Here, the calculation was made using two

long single straps in the toroidal direction with toroidal dipole phasing (0, π). It is clear that in the first case the spectrum peaks at the centre ($n_y = 0$) has the highest contribution. However, in the second case, $n_y = 0$ contribution is null and the contribution of lower even harmonics is reduced. Since the antenna electrical length is not exactly $= \lambda/2$, contribution of higher even harmonics is not reduced. We remark the radiation resistance does indeed decrease in such a case, but the reduction is not dramatic. Since the antenna becomes $> \lambda/4$ at higher frequencies, this loss in coupling is partially compensated by the increase in coupling with frequency due to increase in $k_\perp$ and reduction in the evanescent layer for the same plasma conditions.

4. DISCUSSION AND CONCLUSIONS.

In this paper, we have presented an ICRF antenna physics design for the next-step tokamak for operation at a number of frequencies in a rather large band. Traditionally, ICRF antennas have been designed such that $\beta L \leq \lambda/4$. We have chosen a long length of the antenna (which is possible to accommodate in the next-step devices) such that its electric length $= \lambda/4$ at about 11 MHz but it will become multiples of $\lambda/4$ in the frequency range of interest (20-85 MHz). As mentioned in the last section, there is some loss of coupling at even poloidal mode numbers due to the current reversal when $\beta L > \lambda/4$ but this problem does not appear to be critical. In order that these higher resonances appear at expected frequencies, the antenna has to be constructed such that it acts practically as an ideal strip-line. Often, in the present designs, due to engineering considerations, the antenna loses its short-circuited strip-line identity and the antenna behaves more like a lumped circuit. In such a case, the input impedance response shows a good behaviour up to a frequency such that $L \leq \lambda/4$ but at higher frequencies it departs more and more from the short-circuited strip-line characteristics. As mentioned before, we have neglected the effect of the finite length of the antenna which can also effect the reactive part of the antenna impedance. This must be taken into account in the final design. The actual dimensions of the antenna chosen here are for illustrative purposes and an optimisation must await freezing of the related plasma and machine parameters of the next-step device. In our design the the short section should not be reduced too much (from our value of $L_2 = 0.4$m) as then it starts to short-circuit input impedance completely as well as the current on this section becomes excessively high.

We have only dealt with a traditional antenna with an electrostatic screen. However, if the screenless antenna becomes a viable solution for the next step, the extra capacitance may be provided by extra screen-like metallic strips under the central conductor at appropriate locations. An ICRF antenna system in the next step devices will constitute several modules of an array of 4 or 6 strap especially for the current drive applications. Although we have restricted to treating a single strap but our treatment is also valid for an array as matching is done for each strap separately. In this case appropriate mutual coupling between the straps of the array must be taken into account.

In **conclusion,** a new and improved physics design of an ICRF antenna is presented in which the addition of a short section of strip-line connected in parallel with the main long section of the strip-line antenna improves the coupling resistance at desired frequencies at the low end of the band. This reduces the voltage in the feeder line that must be applied to couple a given amount of power. The presence of this short section serves an additional important function of supporting the central conductor of the feeding line thus alleviating the need of a ceramic support near the antenna in the harsher neutron environment of a reactor. We note that although the voltage in the feeder line is improved, the effect of this short section in any improvement of the maximum antenna voltage is only marginal. The antenna voltage can generally be reduced by increasing the radiation resistance itself i.e. bringing the plasma closer to the antenna, or with the larger depth of the antenna.

ACKNOWLEDGEMENTS.

It is a pleasure to acknowledge the discussion that one of us (JJ) had with Dr P-H. Rebut on the need of a wide-band ICRF antenna for ITER, from where the idea of a "Violin antenna" emerged leading to the present multiple resonance, asymmetrically excited antenna.

REFERENCES.

[1] JACQUINOT J., BURES, M., JET Team, Phys Fluids, B 4 (1992) 2111.
[2] KOCH, R., VAN EESTER, D., Nucl. Fusion, 29 (1989) 59.
[3] KAYE, A., BROWN, T., BHATNAGAR, V.P. et al., Present and Future JET ICRF Antennae, Rep. JET-P(92)46, JET Joint Underatking, Abingdon, Oxfordshire (1992).
[4] WESNER, F., BAUMLER, J., BECKER, W., et al., (Proc. 16th symp. on Fusion Technology, London, 1990), Fusion Technology, North Holland, vol. 2 (1990) 1181.
[5] VAN OOST, G., BHATNAGAR, V.P., DELVIGNE, T., et al., Fusion Technology, 12 (1987) 449.
[6] BAITY, F.W., GOULDING, R.H., HOFFMAN, D.J., et al., (Proc. 16th symp. on Fusion Technology, London, 1990), Fusion Technology, North Holland, vol. 2 (1990) 1035.
[7] BONANOS, P., HOSEA, J., NAGY, A., et al., (Proc. 16th symp. on Fusion Technology, London, 1990), Fusion Technology, North Holland, vol. 2 (1990) 1003.
[8] MORIYAMA, S., FUJII, T., SAIGUSA, M., et al., (Proc. 17th symp. on Fusion Technology, Rome, 1992), Fusion Technology, North Holland, vol. 1 (1992) 584.
[9] SHEPARD, T.D., HASTE, G.R., BAITY, F.W., et al., in RF Power in Plasmas, (Proc. 9th Topical Conf., Charleston, SC, 1991), Amer. Inst. of Phys (1991) 142.
[10] HOFFMAN, D.J., BAITY, F.W., BRYAN, W.E., et al., in RF Power in Plasmas, (Proc. 7th Topical Conf., Kissimmee, Florida, 1987), Amer. Inst. of Phys (1987) 302.
[11] BHATNAGAR, V.P., KOCH, R., MESSIAEN, A.M., WEYNANTS, R.R., Nucl. Fusion, 22 (1982) 280.

[12] TEILHABER, K., JACQUINOT, J., Nucl. Fusion, 24 (1984) 541.
[13] MESSIAEN, A.M., KOCH, R., BHATNAGAR, V.P., et al., Heating in Toroidal Plasmas, (Proc. 3rd Joint Varenna-Grenoble Intn symp., Grenoble, 1982), Commission of Eur. Communities, Brussels, vol. 1 (1982) 243.
[14] TFR Group, SAND, F., Nucl. Fusion, 25 (1985) 1719.
[15] RAMO, S., WHINNERY, J.R., VAN DUZER, T., Fields and Waves in Communication Electronics, John Wiley, 1984.
[16] VABRE, J-P., Ligne de Transmission in Technique de l'Ingineur, Section E646-8 (1958), unpublished.

Table 1. Operation frequencies required for various FWCD/H scenarios* in ITER-EDA at $B_\phi = 6$ T on axis.

f(MHz)	FWCD/H Scenarios	Remarks
≈22	e-TTMP/LD Current Drive and/or pure e-heating	The most efficient C.D. scheme (below all ion resonances)
≈43	Heating D/T mixture at $f = f_{CD}$ (with optimum ion heating for ignition)	Easiest route to ignition
≈60	Heating at $f = 2f_{CT}$ (active phase only) or $f = f_{CHe3}$ (active or non-active phase	Can use a deuterium rich mixture to reduce tritium inventory.
≈75	Minority H or He3 C.D. at q = 1 surface	Sawteeth control (Burn control/ash removal)
≈85	Minority heating $f = f_{CH}$ (Active or non-active phase)	Strong damping per pass. Allows low field operation (1.5 T for 22 MHz)

* Note that some of these scenarios (involving H and He3 minority ion) presume that a small concentration of H or He3 in a reacting plasma could be tolerated in the presence of a significant He4-ash. TTMP and LD refer to transit-time magnetic pumping and Landau damping respectively.

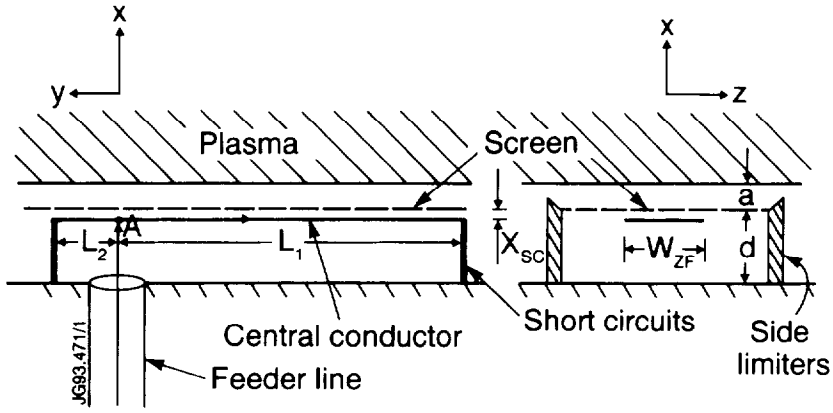

FIG. 1. A schematic diagram of an ICRF antenna constituted by two unequal short-circuited strip-line sections fed in parallel. A feeder-line, an electrostatic screen and side-limiters of such an antenna are also shown schematically.

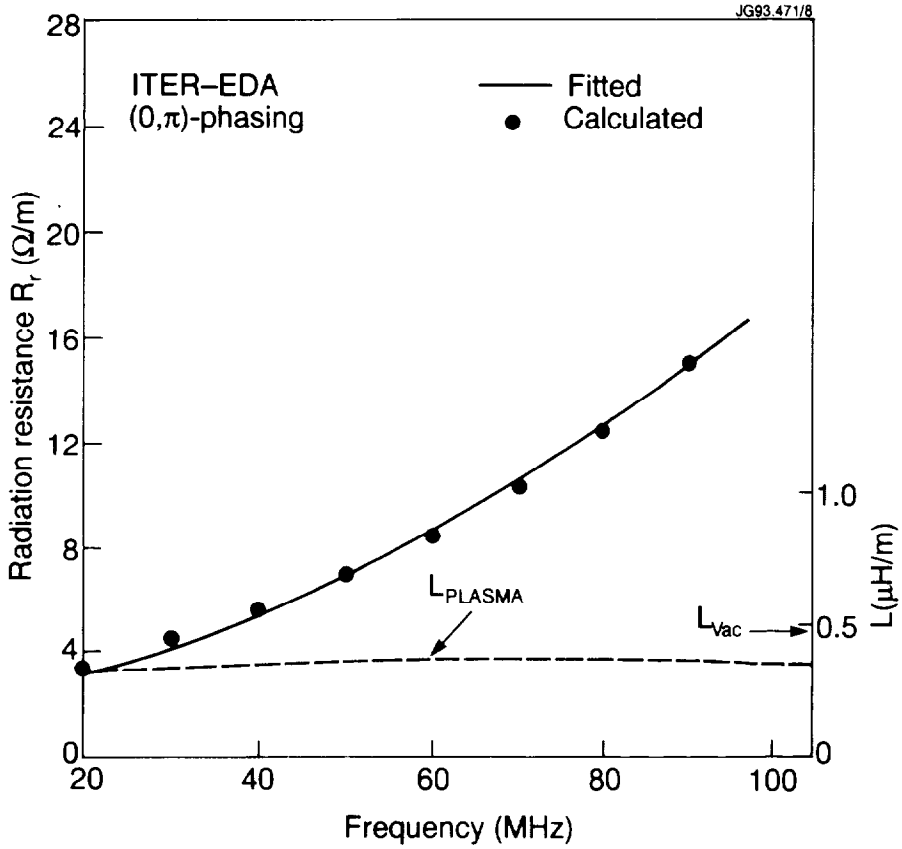

FIG. 2. Radiation resistance R_r versus frequency for an ICRF antenna coupled to a tokamak plasma in dipole (0, π)-phasing for ITER-EDA like parameters: $n_{e0} = 1.4 \cdot 10^{20}m^{-3}$, $n_s = 0.8 \cdot 10^{20}m^{-3}$, 50-50 D/T plasma, $B_\phi 0 = 6T$. The solid symbols represent the calcualtion at discrete frequencies and the line shows the fitted curve with parameters $R_{r0} = 2.5\Omega/m$ and $\alpha_0 = 0.02$ in Eq. 10. The variation of antenna inductance (with plasma) is also shown which is practically constant over the frequency band. The antenna parameters used are given in Section 3.

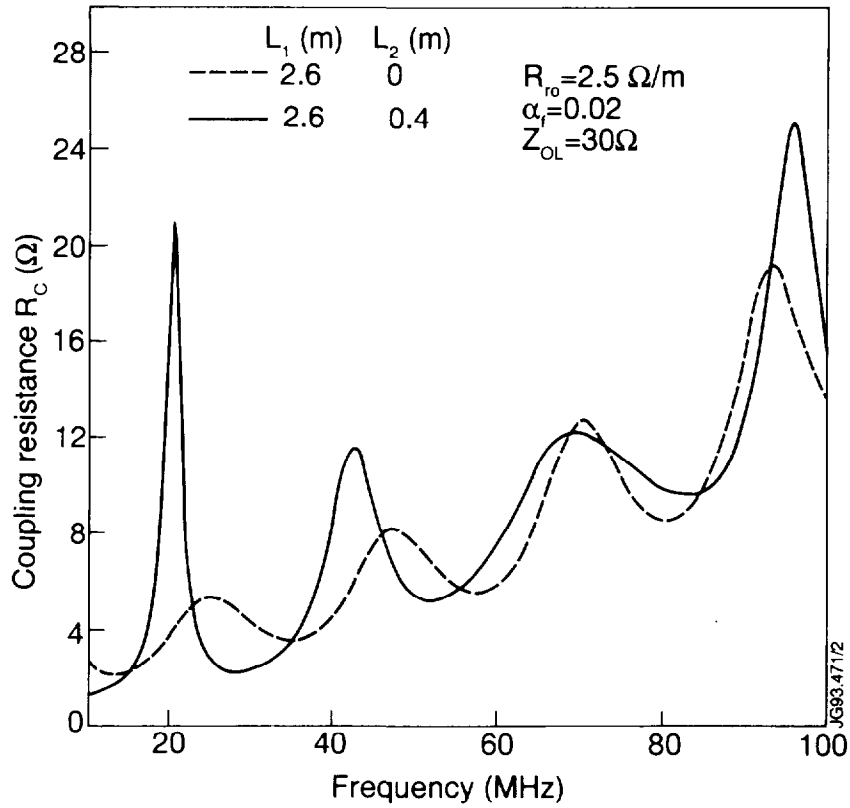

FIG. 3. Plasma coupling resistance R_c versus frequency for an ICRF antenna for two cases (i) two strip lines in parallel with $L_1 = 2.6$m and $L_2 = 0.4$m and (ii) a single strip line with $L = 2.6$ m. In both cases, the connecting feeder line has a $Z_{0L} = 30\Omega$.

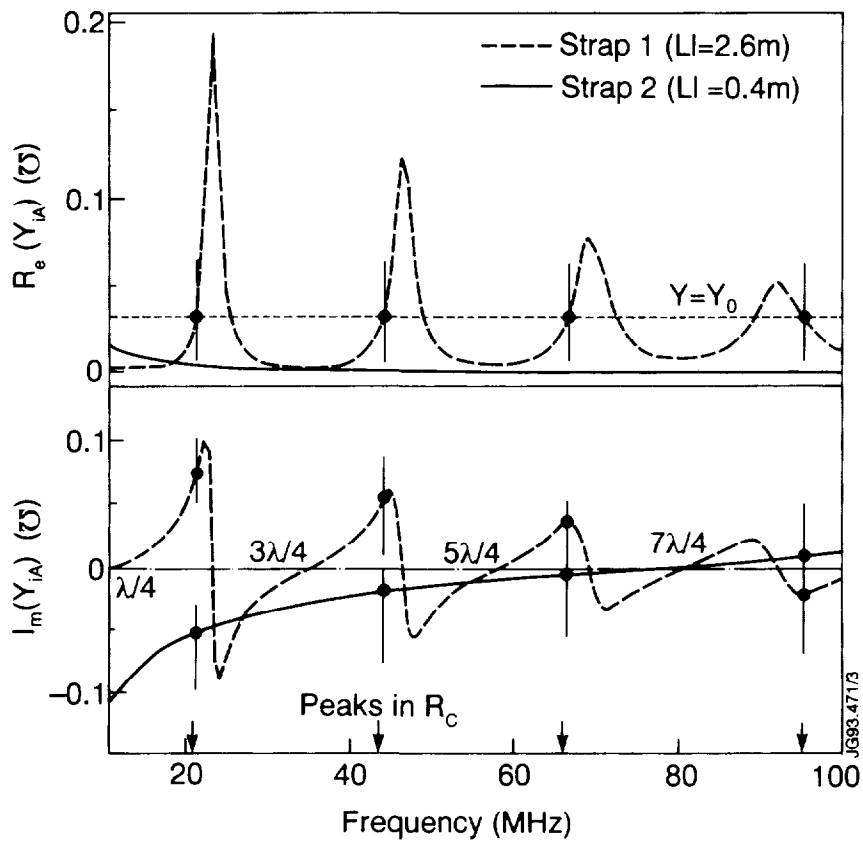

FIG. 4. Real and Imaginary parts of the antenna admittance at the input point A of the two short-circuited strip line sections with $L_1 = 2.6$m and $L_2 = 0.4$m.

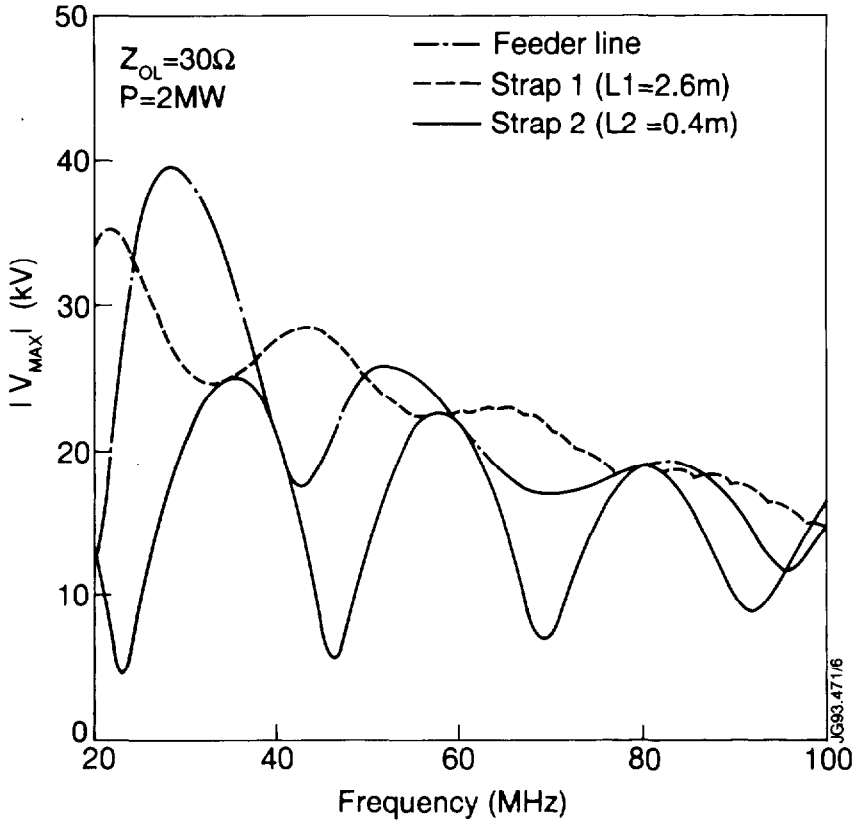

FIG. 5. Magnitude of the maximum voltage in the feeder line and the two sections of the strip line antenna (as in Fig. 3), for example, to deliver a given power of 2 MW, is plotted as a function of frequency.

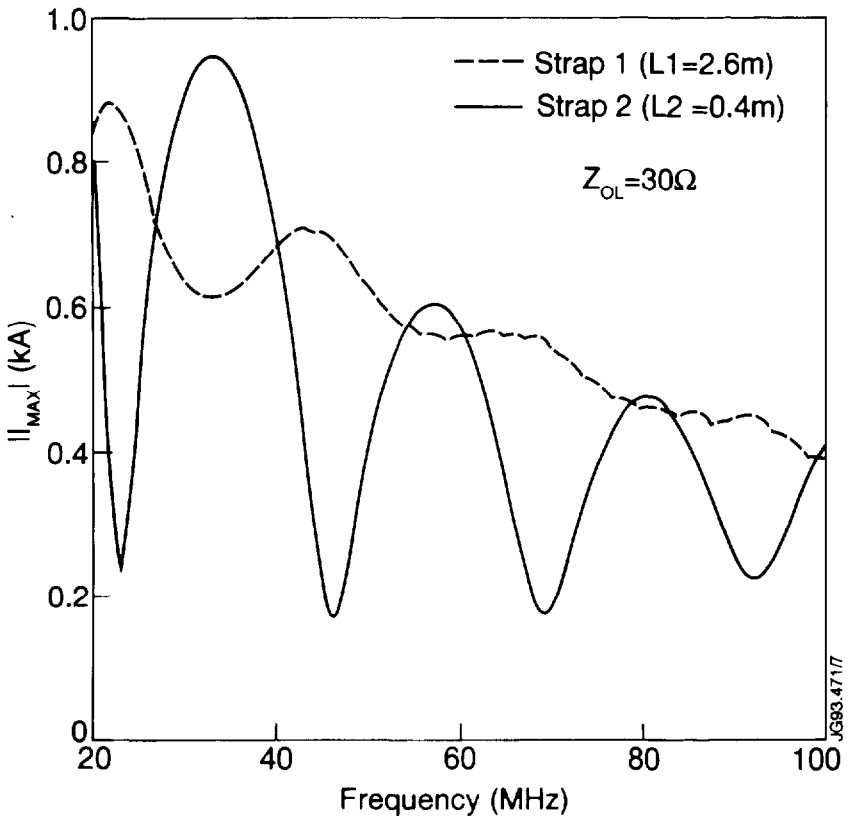

FIG. 6. Magnitude of maximum current versus frequency in the two sections of the strip line antenna corresponding to Fig. 5.

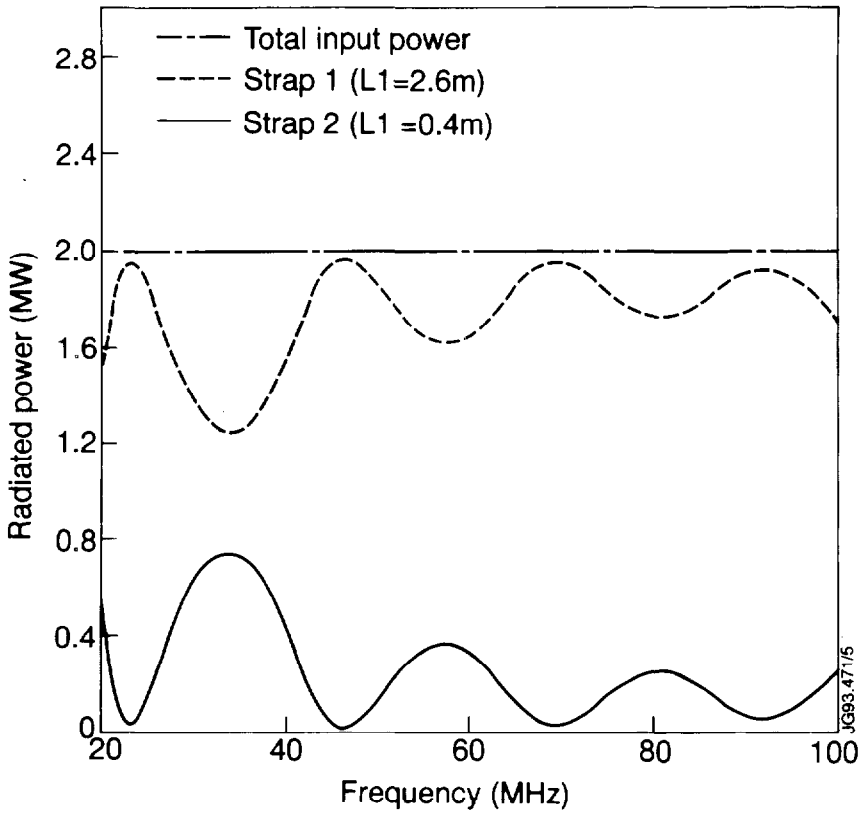

FIG. 7. Power radiated by the two sections of the strip line antenna (as in Fig. 3), with a total input power of 2 MW, is plotted as a function of frequency.

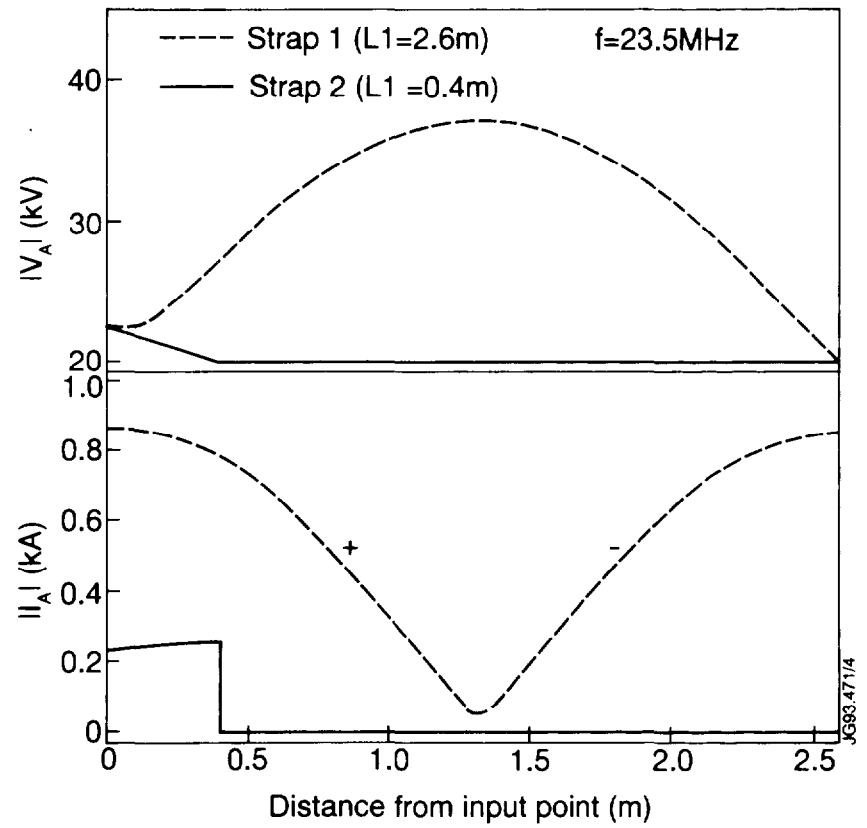

FIG. 8. Voltage and current distribution on the two sections of the strip line antenna at f = 23.5 MHz. Note that the direction of current reverses as the electrical length of the antenna $\beta L > \lambda/4$.

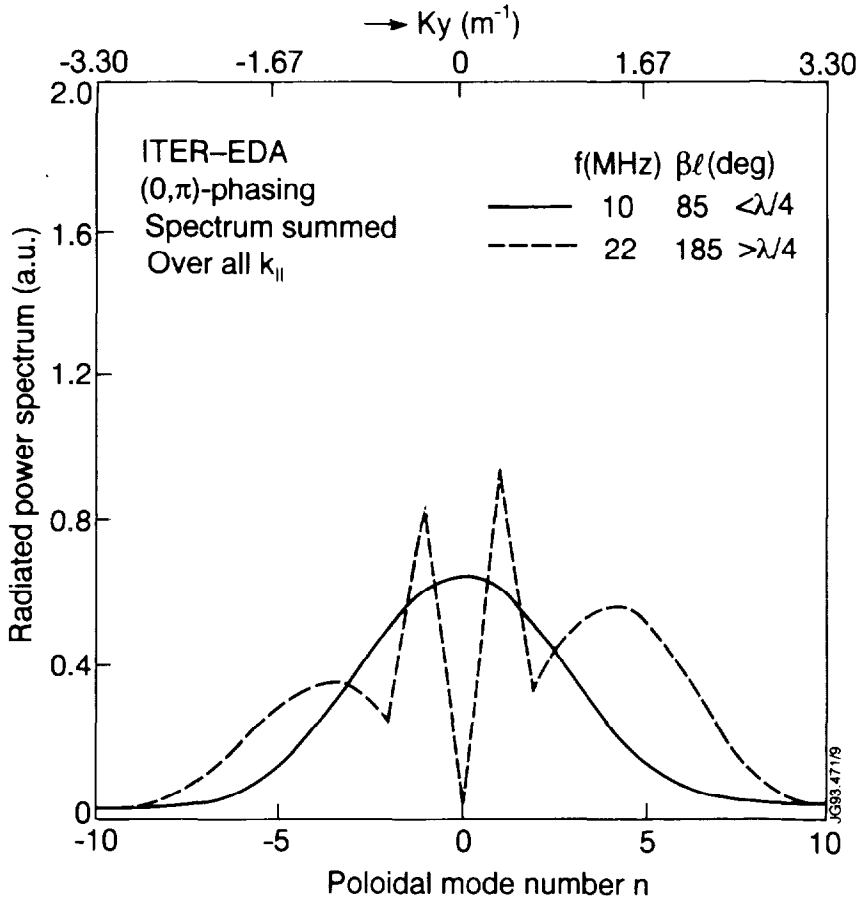

FIG. 9. The radiated power spectrum (with plasma) summed over all $k_{//}$ is plotted as a function of the ploidal mode number at two frequencies (i) f = 10 MHz, $\beta L = 85°$ and (ii) f = 22 MHz, $\beta L = 185°$. Note that in the latter case, coupling for n = 0 ($k_y = 0$) is null and there is decrease of coupling for even mode numbers due to the current reversal on the antenna. Also, $k_y = n/r_A$ where r_A is the minor radius location of the antenna.